Proceedings of ITC-CSCC 2000, Pusan, Korea

# TM scattering by an Elliptic Dielectric Cylinder Loaded Slot

W.J. Byun and N.H.Myung

Department of Electrical Engineering

*Korea Advanced Institute of Science and Technology* (KAIST)

373-1, Kusong-dong, Yusong-gu, Taejon, Korea

*Abstract*— **Analytic series solution for the problem of transverse magnetic (TM) scattering by an elliptic dielectric cylinder loaded slot is presented for an electric line source illumination. The solution is based on using Mathieu functions and mode matching technique (MMT) and it converges very fast.**

## I. Introduction

There have been many studies of sattering by a slot which is loaded by a dielectric circular cylinder in an infinite conducting plane or double wedges [1-3]. However, for many practical applications such as microwave lens antenna, the effect of the shape of the cylinder becomes significant. In this paper, an analytic series solution for the scattering by an elliptic dielectric loaded slot is presented. The slot is loaded with a dielectric cylinder of eccentricity $e$ and wave number $k_2(=\omega\sqrt{\mu_0\epsilon_r\epsilon_0})$. Using Mathieu functions[4] and MMT, we investigate electromagnetic scattering by an elliptic cylinder loaded slot for electric line source illumination.

## II. Field representations

The problem is formulated with respect to elliptic cylinder coordinates $\zeta$, $\eta$ as shown in Fig. 1. $x = d\cosh\zeta\cos\eta$, $y = d\sinh\zeta\sin\eta$and $d$ is semi-

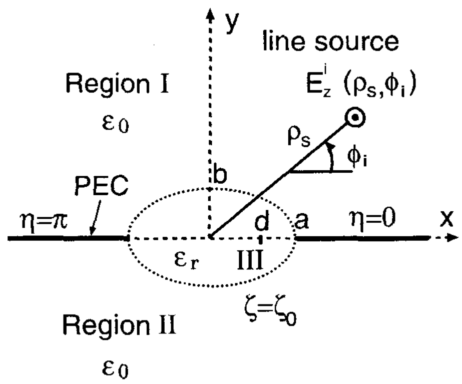


Fig. 1. Geometry of the elliptic dielectric cylinder loaded slot

focal distance. The interface between Regions I, II and III in Fig. 1 is represented by the relation $\zeta_0$ ($e = \frac{1}{\cosh\zeta_0} = \frac{d}{a}$). The eccentricity $e$ is represented by $\sqrt{1-(b/a)^2}$. $a$ and $b$ are semi-major and semi-minor axis, respectively. When the $TM_z$ line source at $(\rho_s, \phi_i)$ impinges on the slot in a PEC, the incident and specularly reflected fields for Region I ($\zeta > \zeta_0, 0 < \eta < \pi$) may be represented as following.

$$E_z^i(\zeta,\eta) \quad + \quad E_z^r(\zeta,\eta) = E_0^l\sum_{p=1}^{\infty}$$

$$
\begin{cases} s_p^{inc} Ms_p^{(1)}(\zeta_s, q_1) Ms_p^{(4)}(\zeta, q_1) \\ \quad se_p(\eta, q_1) \;\; \zeta > \zeta_s \\ s_p^{inc} Ms_p^{(1)}(\zeta, q_0) Ms_p^{(4)}(\zeta_s, q_1) \\ \quad se_p(\eta, q_1) \;\; \zeta < \zeta_s, \end{cases} \tag{1}
$$

where

$$
\begin{aligned}
\cosh\zeta_s &= \left[\frac{1}{2}(\frac{\rho_s^2}{d^2}+1) + \left\{\frac{1}{4}(\frac{\rho_s^2}{d^2}+1)^2 - \frac{\rho_d{}^2}{d^2}\right\}^{\frac{1}{2}}\right]^{\frac{1}{2}} \\
\cos\eta_s &= \left(\frac{\rho_d}{d\cosh\zeta_s}\right) \\
s_p^{inc} &= 4se_p(\eta_s, q_1) \\
E_0^l &= -\frac{k_1^2 I_e}{4\omega\varepsilon_0}
\end{aligned}
$$

where $\rho_d = \rho_s \cos\phi_i$ and $I_e$ is the strength of the electric current filament and $k_1(=\omega\sqrt{\mu_0\epsilon_0})$ is the wave number in the Region I. $Ms_p^{(s)}$, $Mc_p^{(s)}$ for $s = 1, 2$ and 4 are the odd and even radial Mathieu functions of the $sth$ kind and $Ms_p^{(4)} = Ms_p^{(1)} - jMs_p^{(2)}$. The scattered field in Region I may be represented by imposing boundary condition on the PEC substrate since $se_p(\eta, q_1) = 0$ at $\eta = 0$ and $\pi$ as follow,

$$
E_z^s(\zeta,\eta) = E_0^l \sum_{p=1}^{\infty} A_p Ms_p^{(4)}(\zeta, q_1) se_p(\eta, q_1) \tag{2}
$$

The total field in Region I, the scattered field inside the dielectric elliptic cylinder in Region II ($\zeta > \zeta_0, \pi < \eta < 2\pi$) and the transmitted field in Region III ($\zeta < \zeta_0$, $0 < \eta < 2\pi$) may be represented as

$$
\begin{aligned}
E_z^I(\zeta,\eta) &= E_z^i(\zeta,\eta) + E_z^r(\zeta,\eta) + E_z^s(\zeta,\eta) \quad (3) \\
E_z^{II}(\zeta,\eta) &= E_0^l \sum_{p=1}^{\infty} D_p Ms_p^{(4)}(\zeta, q_1) se_p(\eta, q_1) \quad (4) \\
E_z^{III}(\zeta,\eta) &= E_0^l \sum_{n=0}^{\infty} B_n Mc_n^{(1)}(\zeta, q_2) ce_n(\eta, q_2) \\
&+ E_0^l \sum_{n=1}^{\infty} C_n Ms_n^{(1)}(\zeta, q_2) se_n(\eta, q_2) \quad (5)
\end{aligned}
$$

where $q_i = (k_i ae)^2/4$ and $i = 1, 2$. From Maxwell's equations, the $\eta$ -components of the magnetic field may be represented as

$$
H_\eta^{I,II,III} = -\frac{j\omega\epsilon_r}{k_r^2 L}\frac{\partial E_z^{I,II,III}}{\partial\zeta} \tag{6}
$$

where $L = d(\cosh^2\zeta - \cos^2\eta)^{\frac{1}{2}}$ and r=1, 2 for $k_r$ and $\varepsilon_r$, respectively.

In the above equations, $A_p$, $B_n$, $C_n$ and $D_p$ are unknown coefficients to be determined with field continuity conditions across the slot at $\zeta_0$.

$$
\begin{cases} E_z^I = E_z^{III} \\ H_\eta^I = H_\eta^{III} \end{cases}, \quad (\zeta = \zeta_0,\ 0 < \eta < \pi) \tag{7}
$$

$$
\begin{cases} E_z^{II} = E_z^{III} \\ H_\eta^{II} = H_\eta^{III} \end{cases}, \quad (\zeta = \zeta_0,\ \pi < \eta < 2\pi) \tag{8}
$$

Applying the orthogonality condition of the angular Mathieu functions and multiplying $se_p(\eta, q_1)$, the following equations can be obtained for $m$ and $p \geq 1$.

$$
\begin{aligned}
&\sum_{n=0}^{\infty} B_n Mc_n^{(1)}(\zeta_0, q_2) f_{pn12}^{(2)} + \sum_{n=1}^{\infty} C_n Ms_n^{(1)}(\zeta_0, q_2) f_{pn12}^{(1)} \\
&= A_p Ms_p^{(4)}(\zeta_0, q_1) + \hat{s}_p^{inc} Ms_p^{(1)}(\zeta_0, q_1) \quad (9)
\end{aligned}
$$

$$
\begin{aligned}
\sum_{n=0}^{\infty} B_n Mc_n^{(1)}(\zeta_0, q_2) f_{pn12}^{(2)} &- \sum_{n=1}^{\infty} C_n Ms_n^{(1)}(\zeta_0, q_2) f_{pn12}^{(1)} \\
&= -D_p Ms_p^{(4)}(\zeta_0, q_1)\frac{\pi}{2} \quad (10)
\end{aligned}
$$

$$
\begin{aligned}
\sum_{p=1}^{\infty} \Big\{ A_p Ms_p^{(4)\prime}(\zeta_0, q_1) &+ \hat{s}_p^{inc} Ms_p^{(1)\prime}(\zeta_0, q_1) \Big\} f_{mp21}^{(1)} \\
&= \sum_{n=0}^{\infty} B_n Mc_n^{(1)\prime}(\zeta_0, q_2) f_{mn22}^{(2)} \\
&+ C_m Ms_m^{(1)\prime}(\zeta_0, q_2)\frac{\pi}{2}\delta_{mn} \quad (11)
\end{aligned}
$$

$$
\begin{aligned}
C_m Ms_m^{(1)\prime}(\zeta_0, q_2)\frac{\pi}{2}\delta_{mn} &- \sum_{n=0}^{\infty} B_n Mc_n^{(1)\prime}(\zeta_0, q_2) f_{mn22}^{(2)} \\
&= \sum_{p=1}^{\infty} D_p Ms_p^{(4)\prime}(\zeta_0, q_1) f_{mp21}^{(1)} \quad (12)
\end{aligned}
$$

$$
\begin{aligned}
f_{mnij}^{(1)} &= \int_0^\pi se_n(\eta, q_j) se_m(\eta, q_i) d\eta \quad (13) \\
f_{mnij}^{(2)} &= \int_0^\pi ce_n(\eta, q_j) se_m(\eta, q_i) d\eta \quad (14)
\end{aligned}
$$

where $\hat{s}_p^{inc} = s_p^{inc} Ms_p^{(4)}(\zeta_s, q_1)$. Substitution of Eqs.(9) and (10) into (11) and (12) yields the simultaneous equations in terms of $A_n$ and $B_n$ as following.

$$\begin{bmatrix} \Psi_{11} & \Psi_{12} \\ \Psi_{21} & \Psi_{22} \end{bmatrix} \begin{bmatrix} B_n Mc_n^{(1)}(\zeta_0, q_2) \\ C_n Ms_n^{(1)}(\zeta_0, q_2) \end{bmatrix} = \begin{bmatrix} \Gamma_1 \\ 0 \end{bmatrix} \quad (15)$$

$$\begin{aligned}
\psi_{11,mn} &= \sum_{p=1}^{\infty} MS^{(4)} f_{pm12}^{(2)} f_{mp21}^{(1)} - Mc_n^{(1)'}(\zeta_0, q_2) f_{mn22}^{(2)} \\
\psi_{12,mn} &= \sum_{p=1}^{\infty} MS^{(4)} f_{pm12}^{(1)} f_{mp21}^{(1)} - Ms_m^{(1)'}(\zeta_0, q_2) \frac{\pi}{2} \delta_{mn} \\
\psi_{21,mn} &= -\sum_{p=1}^{\infty} MS^{(4)} f_{mp21}^{(1)} f_{pn12}^{(2)} + Mc_n^{(1)'}(\zeta_0, q_2) f_{mn22}^{(2)} \\
\psi_{22,mn} &= \sum_{p=1}^{\infty} MS^{(4)} f_{mp21}^{(1)} f_{np12}^{(1)} - Ms_m^{(1)'}(\zeta_0, q_2) \frac{\pi}{2} \delta_{mn} \\
\gamma_{1,m} &= \sum_{p=1}^{\infty} \hat{s}_p^{inc} f_{mp21}^{(1)} \Big\{ Ms_p^{(1)}(\zeta_0, q_1) MS^{(4)} \frac{\pi}{2} \\
&\quad - Ms_p^{(1)'}(\zeta_0, q_1) \Big\} \\
MS^{(4)} &= \frac{Ms_p^{(4)'}(\zeta_0, q_1)}{\frac{\pi}{2} Ms_p^{(4)}(\zeta_0, q_1)}
\end{aligned}$$

The unknown coefficients $C_n$ and $D_n$ from Eqs. (9) and (10) are expressed as following.

$$\begin{aligned}
\frac{\pi}{2} A_p Ms_p^{(4)}(\zeta_0, q_1) &= \sum_{n=0}^{\infty} B_n Mc_n^{(1)'}(\zeta_0, q_2) f_{pn12}^{(2)} \\
&+ \sum_{n=1}^{\infty} C_n Ms_n^{(1)}(\zeta_0, q_2) f_{pn12}^{(1)} \\
&- s_p^{inc} Ms_p^{(1)}(\zeta_0, q_1) \frac{\pi}{2} \qquad (16)
\end{aligned}$$

$$\begin{aligned}
\frac{\pi}{2} D_p Ms_p^{(4)}(\zeta_0, q_1) &= -\sum_{n=0}^{\infty} B_n Mc_n^{(1)'}(\zeta_0, q_2) f_{pn12}^{(2)} \\
&+ \sum_{n=1}^{\infty} C_n Ms_n^{(1)}(\zeta_0, q_2) f_{pn12}^{(1)} (17)
\end{aligned}$$

The infinite series involved in the solution are convergent, and this makes it possible to truncate after a certain number of terms to determine the unknown coefficients $B_n$ and $C_n$. Once $B_n$ and $C_n$ is determined, it is possible to evaluate $A_p$ and $D_p$ using Eqs. (16) and (17).

## III. Transmitted Field Computation

The analysis has been done for the line source illumination so far, plane wave excitation can be also obtained by letting the line source recede to infinity. The transmission coefficient of the elliptic dielectric loaded slot is the ratio of the time average transmitted through the dielectric interface at $\zeta = \zeta_0$ and $180^o < \eta < 360^o$ into the lower sector to the time average power produced by the plane wave source, represented by

$$T = \frac{1}{2ka} \sum_{p=1}^{N} |D_p|^2 \qquad (18)$$

Fig. 2 shows the change of the transmission coefficients for loaded slot with frequency and eccentricities ($b = a$, $0.86a$ and $0.3a$). It is noted that $T$ for circular dielectric loaded slot as the limiting case of elliptic one agrees well with the transmission coefficient of [2].

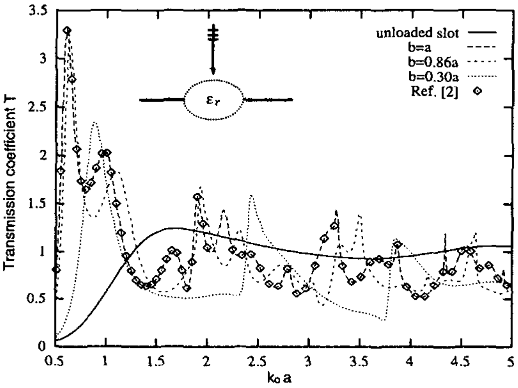


Fig. 2. Change of transmission coefficient vs. $k_0 a$ for plane wave incidence with different eccentricities, $\phi_i = 90^o$ and $\epsilon_r = 5$

When the observation is located at far distance, the transmitted field at Region II can be written as

$$\begin{aligned}
Ms_p^{(4)} &\overset{\zeta \to \infty}{\simeq} \sqrt{\frac{2}{\pi k_1 d \sinh\zeta}} e^{-j(k_1 d \sinh\zeta - \frac{(2p+1)\pi}{4})} \\
d \sinh\zeta &\overset{\zeta \to \infty}{\simeq} \rho \\
E_z^{II}(\zeta, \eta) &\overset{\zeta \to \infty}{\simeq} E_0^l \sqrt{\frac{2}{\pi k_0 \rho}} e^{-j(k_0 \rho - \frac{\pi}{4})} F(\eta, q_1)
\end{aligned}$$

$$F(\eta, q_1) = \sum_{p=1}^{N} (j)^p D_p se_p(\eta, q_1) \quad (19)$$

Transmitted far field pattern is shown in Fig. 3 for line source illumination ($\rho_s = 1\lambda, \phi_i = 90^o, \epsilon_r = 1, 3, 5$ and 7) with the eccentricity fixed. Fig. 4 shows transmitted far field pattern for plane wave incidence ($\phi_i = 90^o$, $\epsilon_r = 1, 3, 5$ and 7) with the different eccentricities ($e = 1/\sqrt{\epsilon_r}$). It is also known from optics that the geometric focus becomes the optical focus for a given index of refraction $n = \sqrt{\epsilon_r}$ [5]. It is noted that one can obtain a flat-topped pattern at $\epsilon_r = 3$.

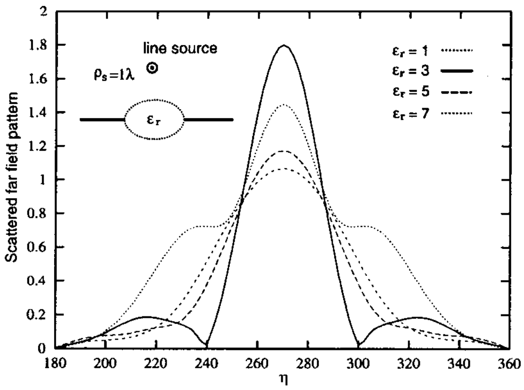


Fig. 3. Scattered far field patterns for elliptic cylinder loaded slot vs. $\epsilon_r$ for a line source illumination ($\rho_s = 1\lambda, \phi_i = 90^o$), $a = 1\lambda$ and $b = 0.5\lambda$

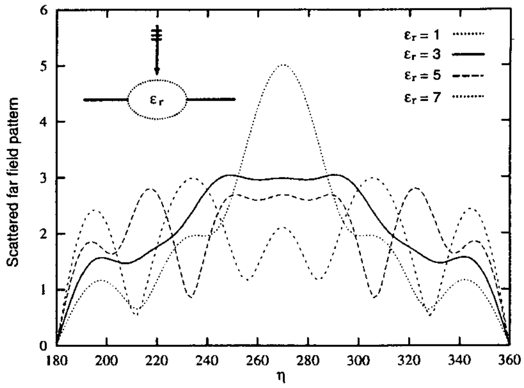


Fig. 4. Scattered far field patterns for elliptic cylinder loaded slot vs. $\epsilon_r$ for plane wave incidence ($\phi_i = 90^o$) and $e = {\epsilon_r}^{-1/2}$

## IV. Conclusion

An analytic series solution for the problem of transverse magnetic wave scattering by a elliptic dielectric loaded slot is presented in this paper. Examination of our results shows that the eccentricities of the dielectric cylinder lead to significant variation in the transmitted far field pattern.

## References


[1] R.A.Hurd and B.K.Sachdeva, "Scattering by a dielectric loaded slit in a conducting plane," *Radio Sci.*, vol.10, pp.565-572, 1975.

[2] A.Z.Elsherbeni and H.A.Auda, "Electromagnetic diffraction by two perfectly conducting wedges with dented edges loaded with a dielectric cylinder," *IEE Proc.* , vol. 136, Pt. H, no. 3, pp.225-234, June, 1989.

[3] J.W.Yu and N.H.Myung, "Scattering by a dielectric loaded nonplanar slit-TM case," *IEEE Trans. Antennas and Prop.*, vol.46, no.4, pp.598-600, Apr., 1998.

[4] N.W.McLachlan, *Theory and Applications of Mathieu Functions*, Dover, New York, 1964.

[5] E. Hecht, *Optics, 2nd edition*, Addison-Wesley pp.128-131, 1987.